Journal of Thermal Analysis and Calorimetry, Vol. 73 (2003) 323–331

EFFECT OF RAPID SOLIDIFICATION ON HEAT CAPACITIES OF Al–Sr ALLOYS

Y. Wang[1], *Z. Zhang*[2*], *X. Bian*[2] *and J. Zhang*[2]

[1]School of Materials Science and Engineering, Jinan University, 106 Jiwei Road, Jinan 250022 P. R. China
[2]The Key Laboratory of Liquid Structure and Heredity of Materials, Shandong University 73 Jingshi Road, Jinan 250061, P. R. China

(Received November 5, 2002; in revised form January 15, 2003)

Abstract

Heat capacities of both the ingot-like and melt-spun Al–Sr alloys have been measured through the temperature range 373 to 1060 K using differential scanning calorimetry. The experimental results show that rapid solidification has a slight effect on the temperature dependence of the heat capacities of the Al–Sr alloys. The heat capacities of the melt-spun Al–Sr alloys increase more slowly than those of the ingot-like alloys with increasing temperature from 373 to 900 K. Furthermore, the effect of rapid solidification on the heat capacities becomes more obvious with increasing Sr concentration in the Al–Sr alloys. The data of the heat capacities between 373 and 900 K have been fitted with the least square method and a linear dependence on temperature was assumed for that temperature range.

Keywords: Al–Sr alloys, differential scanning calorimetry, heat capacity, rapid solidification

Introduction

Al–Sr alloys are widely used in industrial practice for the modification of Al–Si alloys, by which the eutectic Si is converted from a coarse flake into a fine fibrous morphology [1–3]. Sr has a low oxidation sensitivity and its use leads to the elimination of two major problems associated with Na modification, namely, fume generation and control of the amount of addition. These have led towards a growing importance of Sr as a strong modifier [4] and much attention has been paid to the determination of phase diagram [5, 6], preparation [7], modification efficiency [8], and viscosity [9] of Al–Sr alloys.

The heat capacity C_p is one of the most fundamental thermodynamic properties of matter. Based on the known data of the temperature dependence of heat capacities, other thermodynamic functions, such as enthalpy, entropy and Gibbs free energy, can be calculated [10]. Investigations of the heat capacities of solid elements have been made for many years. The theoretical work of Einstein, Debye and others on the heat

* Author for correspondence: E-mail: zh_zhang@sdu.edu.cn

1388–6150/2003/ $ 20.00
Akadémiai Kiadó, Budapest

capacity of a solid element is well known. The values of the heat capacities of liquid alloys have often been estimated by proportional addition of the heat capacities of the constituent elements, i.e. the Neumann-Kopp law [11]. Hoch [12, 13] has calculated the heat capacities of solids, undercooled liquid metals and alloys. Wang *et al.* [10, 14] has measured the heat capacities of intermetallic compounds in the Fe–Ti and Co–Ti systems using differential scanning calorimetry. Several studies have been carried out to investigate the thermodynamics of liquid Al–Sr alloys [15], including the enthalpy of formation [16, 17] and vapour pressure [18, 19]. However, few data are available on the heat capacities of solid and liquid Al–Sr alloys.

Differential scanning calorimetry (DSC) has been used for decades for the characterization of caloric effects of various kinds of samples [20–22]. This technique allows characterization of transformation energetics as well as measurement of heat capacities. DSC combined with an entrained droplet technique [23] has been successfully used on a series of melt-spun alloys with deliberate impurity additions to study the nucleation related aspects of secondary phase selection during solidification of dilute Al alloys [24]. Ramakumar *et al.* [25] proved that reasonably precise and accurate heat capacity measurements are possible with DSC. In our previous work, the heat capacities of superheated Al–10Sr alloy melt have been reported [26]. In this study, the temperature dependence of heat capacities of the Al–Sr alloys has been measured using DSC and the effect of rapid solidification on the heat capacities has been investigated.

Experimental

In this investigation, elemental Al (99.9% purity) and Sr (99.7% purity) were used to prepare alloys of nominal compositions Al–5Sr, Al–10Sr and Al–23Sr (wt.%). The charges were melted in a graphite clay crucible using a medium frequency induction electric furnace under an inert argon atmosphere and were cast into ingots in a copper chill mould. The real compositions of the alloys obtained were analyzed using the atomic absorption technique and presented in Table 1. Using a single roller melt spinning apparatus, the prealloyed ingot was remelted by high-frequency induction heating and rapidly solidified into continuous ribbons at a wheel speed of 1500 revolutions per min (rpm) in a controlled inert atmosphere. The copper roller is 35 cm in diameter. The melt-spun ribbons were typically 3–5 mm in width and 30–50 μm in thickness. The ribbons were characterized using X-ray diffraction (XRD), optical microscopy (OM) and transmission electron microscopy (TEM).

Table 1 Chemical compositions of Al-Sr alloys

Alloys		Al–5Sr	Al–10Sr	Al–23Sr
Nominal composition	wt.%	5	10	23
	at.%	1.6	3.3	8.4
Real composition	wt.%	5.05	9.85	23.52

Heat capacities of both the ingot-like and melt-spun Al–Sr alloys were measured using a differential scanning calorimeter (high-temperature NETZSCH DSC 404). Synthetic sapphire supplied by the manufacturer was used as a standard reference material. Al_2O_3 crucibles (of equal mass) with lids were used for all the tests. The DSC for the heat capacity measurements was initially calibrated for temperature and calorimetric sensitivity. Calibration runs with pure In, Zn, Al and Au standard samples yielded an absolute accuracy in C_p values of better than ±3% compared to the literature values. Samples for the C_p measurements were accurately determined to be 20 mg. Determination of C_p was carried out employing the ratio method [27]. Using this method three measurements under the same test conditions are necessary. Measurements were carried out through the temperature range 373 to 1060 K at a heating rate of 20 K min^{-1}, under an argon atmosphere with a flow rate of 80 mL min^{-1}. Minimum two independent experiments were performed for each sample. The average was taken as the heat capacity of the sample.

Results and discussion

The microstructures of both ingot-like and melt-spun Al–5, 10 and 23 Sr alloys were characterized elsewhere in detail [7, 28–30]. A brief description of the microstructures of Al–Sr alloys is given as follows. According to the binary Al–Sr phase diagram, the eutectic composition is about 3.2 [5] or 2.4 [6] wt.% Sr at the Al-rich end. All the three alloys discussed here are hypereutectic. The microstructures of the ingot-like Al–Sr alloys consist of coarse plate-like primary Al_4Sr, about 20–40 μm in width and 150–300 μm in length, embedded in the α-Al/Al_4Sr eutectic matrix. According to the OM, XRD and TEM results, rapid solidification (RS) has a marked effect on the microstructures of the three Al–Sr alloys, but no effect on the phase constituents. OM observations show that the cross section of the Al–5Sr ribbons is duplex cellular. TEM results show that the microstructure of the melt-spun Al–5Sr alloy is hypoeutectic and composed of fine cellular primary α-Al phase and the ultrafine α-Al/Al_4Sr eutectic [29]. For the Al–10Sr alloy, a completely eutectic microstructure is observed under RS conditions. Moreover, the eutectic microstructure is nanoscale and the eutectic Al_4Sr is less than 40 nm in size [28]. A featureless microstructure was observed under OM, as shown in Fig. 1. For the melt-spun Al–23Sr alloy, the microstructure is composed of primary Al_4Sr dendrites embedded in the α-Al matrix. Furthermore, RS has a significant effect on the morphologies and crystallographic preferred orientations of primary Al_4Sr [30]. Figure 2 shows the microstructures of the ingot-like Al–23Sr and melt-spun Al–10Sr alloys.

Figure 3 shows the heat capacities of the Al–Sr alloys through the temperature range 373 to 1060 K. On the whole, the heat capacities of both the ingot-like and melt-spun alloy gradually increase with increasing temperature before melting, although the heat capacities show slightly decreases at lower temperatures. With temperature exceeding 900 K, the heat capacities sharply increase to a very high value due to melting and then sharply decrease by the end of melting. It can also been seen from Fig. 3 (a), (b) and (c) that rapid solidification has a slight effect on the heat capacities of the Al–Sr alloys. The heat capacities of the melt-spun Al–5Sr alloy in-

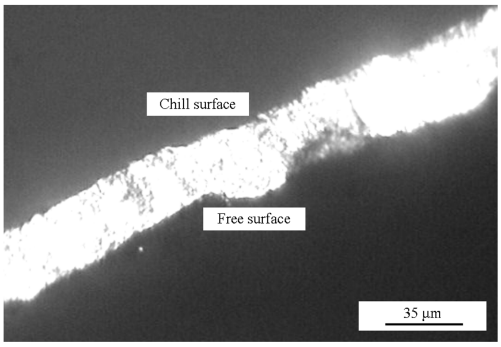

Fig. 1 OM image showing the cross section of the melt-spun Al–10Sr ribbons

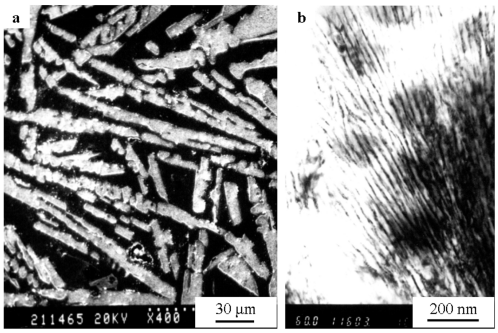

Fig. 2 Microstructures of the ingot-like Al–23Sr (a – SEM) and melt-spun Al–10Sr (b – TEM)

crease more slowly with increasing temperature in comparison with those of the ingot-like alloy, as seen in Fig. 3 (a). The similar tendency can also be seen for the Al–10Sr and Al–23Sr alloy, seen in Fig. 3 (b) and (c) respectively. Furthermore, the higher Sr concentration in the alloys is, the more obvious the tendency is. To clearly show the temperature dependence of heat capacity before melting, the enlarged plots are presented as insets in Fig. 3. The insets show clearly the effect of rapid solidification on the heat capacities of the Al–Sr alloys.

The data of heat capacity are usually fitted by the following functions

$$C_p = a + bT \tag{1}$$

$$C_p = a + bT + cT^{-1} \tag{2}$$

$$C_p = a + bT + cT^{-2} \tag{3}$$

$$C_p = a + bT + cT^{-2} + dT^2 \tag{4}$$

where T is the absolute temperature in K, a, b, c, and d are parameters. In the present case, emphasis is put on the temperature dependence of the heat capacities of the

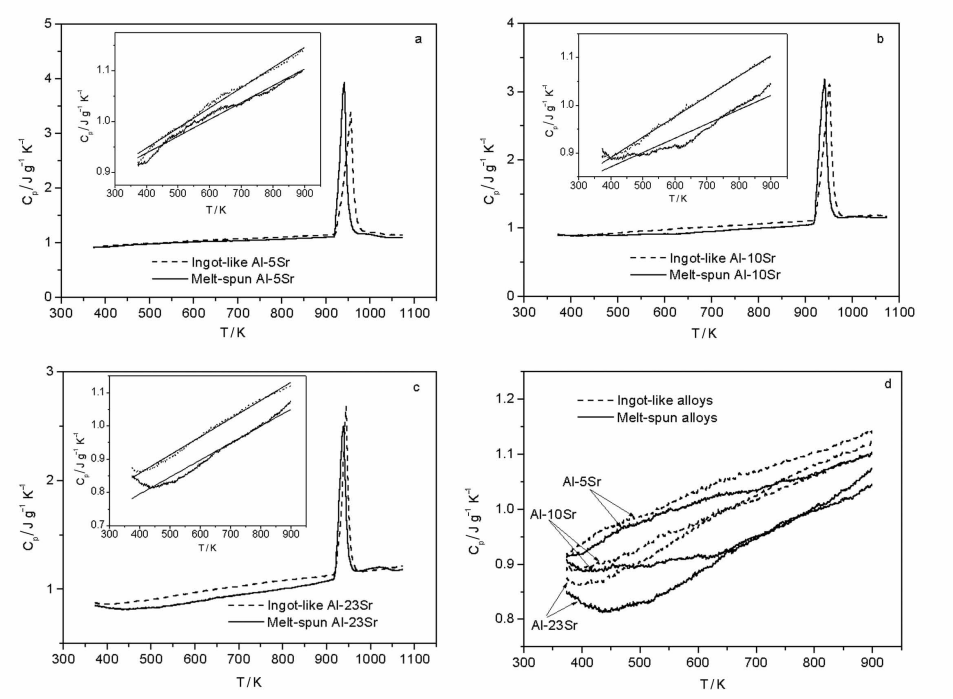

Fig. 3 Heat capacities of the Al–Sr alloys. Fig. 3d and insets in Fig. 3 a – , b – and c – show the heat capacities of Al–Sr alloys from 373 to 900 K. The fitted lines according to Eq. (1) are presented in the insets (solid lines)

Al–Sr alloys through the temperature 373 to 900 K (before melting). Therefore, the Eq. (1) is mainly used to fit the heat capacities of the Al–Sr alloys with the least square method. The fitted lines are presented as solid lines in the insets of Fig. 3 (a), (b) and (c) for the Al–5Sr, Al–10Sr and Al–23Sr respectively. The fitted results are tabulated in Table 2. As a whole, the heat capacity shows a linear relationship with the temperature and the fitted lines serve to describe the temperature dependence of the heat capacities of the Al–Sr alloys between 373 and 900 K, especially for the ingot-like alloys. For the melt-spun Al–Sr alloys, however, the fitted lines are not ideal in spite of sufficiently describing the variation tendency of the heat capacity. The Eq. (4) is also used to fit the heat capacity of the melt-spun Al–10 and 23Sr alloys. The fitted results are shown in Fig. 4 and Table 3. It can be seen that the fitted curves well serve to describe the temperature dependence of the heat capacity.

The variance ratio of the heat capacity with temperature can be indicated by the first derivative of the heat capacity C_p with respect to temperature T, b, namely the slope of the fitted lines. As seen in Table 2, the values of b for the melt-spun Al–Sr alloys are less than those for the ingot-like alloys, indicating that the heat capacities of

Table 2 Parameters in Eq. (1)

Alloys	a/J g^{-1} K^{-1}	b/J g^{-1} K^{-2}
Ingot-like Al–5Sr	0.78882±0.00112	0.00040±2·10^{-6}
Melt-spun Al–5Sr	0.80533±0.00141	0.00033±2·10^{-6}
Ingot-like Al–10Sr	0.71999±0.00066	0.00043±1·10^{-6}
Melt-spun Al–10Sr	0.75137±0.00265	0.00030±4·10^{-6}
Ingot-like Al–23Sr	0.63977±0.00131	0.00055±2·10^{-6}
Melt-spun Al–23Sr	0.59201±0.00323	0.00051±5·10^{-6}

the melt-spun alloys increase more slowly than those of the ingot-like alloys. Figure 3(d) shows the effect of alloy composition on the temperature dependence of the heat capacity of the Al–Sr alloys. It can be seen that the heat capacity increases more rapidly with increasing Sr concentration in the Al–Sr alloys. At a certain temperature, however, the heat capacity slightly decreases with increasing Sr concentration.

To further show the effect of rapid solidification on C_p, ΔC_p is defined as the difference in heat capacity between the ingot-like and melt-spun Al–Sr alloys. Figure 5 shows the plots of ΔC_p *vs*. T. For the Al–5Sr alloy, ΔC_p slowly increases with increasing temperature indicating that the effect of rapid solidification on C_p is more obvious with temperature. For the Al–10 and 23Sr alloys, however, ΔC_p first increases and then decreases with increasing temperature. At a certain temperature, ΔC_p increases with increasing Sr concentration in the Al–Sr alloys. In other words, the effect of rapid solidification on C_p becomes more obvious with increasing alloy composition.

According to the results mentioned above, rapid solidification has a slight effect on the temperature dependence of the heat capacities of the Al–Sr alloys through the temperature range 373 to 900 K. In the previous work, it was reported that the increase of the heat capacity of the liquid Al–10Sr alloy with the temperature exceeding 1300 K is due to the disappearance of atomic clusters and the disordering of the liquid

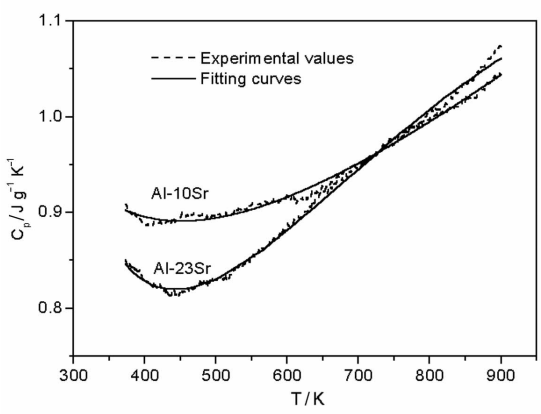

Fig. 4 Heat capacities of the melt-spun Al–10 and 23Sr alloys

Table 3 Parameters in Eq. (4)

Alloys/wt.%	a/J g^{-1} K^{-1}	b/J g^{-1} K^{-2}	c/J g^{-1} K	d/J g^{-1} K^{-3}
Melt-spun Al–10Sr	0.71777±0.0231	0.00009±5·10^{-5}	15202±1249	2.765·10^{-7}±3·10^{-8}
Melt-spun Al–23Sr	–0.35909±0.0239	0.00232±5·10^{-5}	65210±1291	–9.259·10^{-7}±3·10^{-8}

structure [26]. The anomalous increase of heat capacity of the Ni–Pd alloys at high temperatures was explained by the disordering of a chemical short-range order [31]. Nevertheless, formation of short-range order and clustering requires a thermally activated process starting from a metastable state and a depression of heat capacity. Under conventional solidification conditions, the microstructures of the Al–Sr alloys used in this investigation are composed of the coarse plate-like primary Al_4Sr and the eutectic matrix [7]. The heat capacities of the ingot-like Al–Sr alloys slowly increase with increasing temperature up to 900 K due to the enhancement of lattice vibrations. Under rapid solidification conditions, however, the microstructures of the Al–Sr alloys are quite different from those of the ingot-like alloys. For example, a completely eutectic microstructure with the Al_4Sr size less than 40 nm was obtained in the

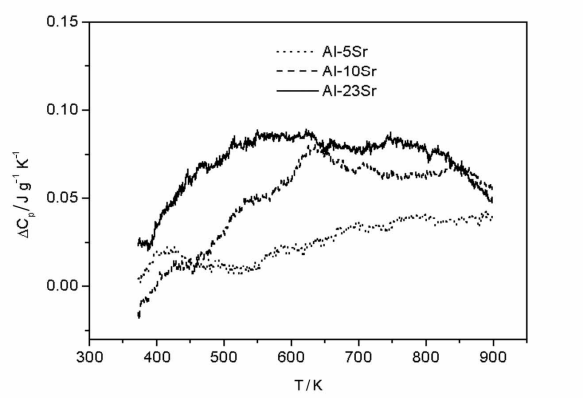

Fig. 5 Plots of $\Delta_p C_p$ *vs. T*

melt-spun Al–10Sr alloy [28]. The nanoscale eutectic microstructure is metastable and will transform into the stable state with increasing temperature. In other words, the ultrafine Al_4Sr phase will grow up with temperature. The growth of the Al_4Sr phase and the coarsening of the microstructure give rise to the slow increase of the heat capacities of the melt-spun Al–Sr alloys with temperature, compared to the ingot-like alloys. Moreover, the volume fraction of Al_4Sr phase increases with increasing Sr concentration in the Al–Sr alloys. Therefore, the effect of rapid solidification on the heat capacities becomes more obvious with increasing Sr concentration in the Al–Sr alloys.

Conclusions

On the whole, the heat capacities of both the ingot-like and melt-spun Al–Sr alloys slowly increase with increasing temperature from 373 to 900 K. Rapid solidification has a slight effect on the temperature dependence of the heat capacities of the Al–Sr alloys. The heat capacities of the melt-spun Al–Sr alloy increase more slowly with temperature compared to those of the ingot-like alloys. Furthermore, the effect of rapid solidification on the heat capacities become more obvious with increasing Sr concentration in the Al–Sr alloys. The growth of the Al_4Sr phase and coarsening of the microstructure of the melt-spun Al–Sr alloys may be responsible for the slower increase of the heat capacities with increasing temperature. The heat capacities of the Al–Sr alloys through the temperature range 373 to 900 K exhibit a linear dependence on temperature according to the fitting on the data of heat capacities with the least square method.

* * *

The authors give grateful thanks for the support of the National Natural Science Foundation of China and Shandong Natural Science Foundation of China, under grant Nos.50071028 and Z2001F02.

References

1 J. Y. Chang and H. S. Ko, J. Mater. Sci. Lett., 19 (2000) 197.
2 B. Heshmatpour, in: R. Huglen (Ed.), Light Metals 1997, TMS, Warrendale, p. 801.
3 D. Emadi, J. E. Gruzleski and J. M. Toguri, Metall. Trans. B, 24 (1993) 1055.
4 M. M. Haque, J. Mater. Proc. Technol., 55 (1995) 193.
5 C. B. Alcock and V. P. Itkin, Bulletin of Alloy Phase Diagrams, 10 (1989) 624.
6 B. Closset, H. Dugas, M. Pekguleryuz and J. E. Gruzleski, Metall. Trans. A, 17 (1986) 1250.
7 Z. H. Zhang, X. F. Bian and X. F. Liu, Z. Metallkd., 92 (2001) 1323.
8 J. Y. Qin, X. F. Bian, X. J. Han, X. F. Liu and J. J. Ma, Chinese J. Mater. Res., 13 (1999) 162.
9 Z. H. Zhang and X. F. Bian, Z. Metallkd., 92 (2001) 1319.
10 H. Wang, R. Lück and B. Predel, Z. Metallkd., 84 (1993) 230.
11 T. Iida and R. I .L. Guthrie, The Physical Properties of Liquid Metals, Clarendon Press, Oxford 1993.
12 M. Hoch, Z. Metallkd., 83 (1992) 820.
13 M. Hoch, Z. Metallkd., 86 (1995) 557.
14 H. Wang and R. Lück, Z. Metallkd., 84 (1993) 627.
15 S. Srikanth and K. T. Jacob, Z. Metallkd., 82 (1991) 675.
16 F. Sommer, J. J. Lee and B. Predel, Z. Metallkd., 74 (1983) 100.
17 Y. O. Esin, V. V. Litovski, S. E. Demin and M. S. Petrushevski, Russ. J. Phys. Chem., 59 (1985) 446.
18 B. P. Burylev, A. V. Vakhobov and T. D. Dzhuraev, Russ. J. Phys. Chem., 48 (1974) 809.
19 A. V. Vakhobov, T. D. Dzhuraev and B. N. Vigdorovich, Russ. J. Phys. Chem., 48 (1974) 1306.
20 J. Blumm and E. Kaisersberger, J. Therm. Anal. Cal., 64 (2001) 385.
21 R. Androsch, J. Therm. Anal. Cal., 61 (2000) 75.

22 T. Mitsuhashi and A. Watanabe, J. Therm. Anal. Cal., 60 (2000) 683.
23 C. C. Wang and C. S. Smith, Trans. Met. Soc. AIME, 188 (1950) 136.
24 C. M. Allen, K. A. Q. O'Reilly, B. Cantor and P. V. Evans, J. Therm. Anal. Cal., 57 (1999) 391.
25 K. L. Ramakumar, M. K. Saxena and S. B. Deb, J. Therm. Anal. Cal., 66 (2001) 387.
26 Y. Wang, X. F. Bian, Z. H. Zhang and Y. M. Sun, Trans. Non-ferrous Met. Soc. China, 11 (2001) 455.
27 J. B. Henderson, W.-D. Emmerich and E. Wassmer, J. Thermal Anal., 33 (1988) 1067.
28 Z. H. Zhang, X. F. Bian and Y. Wang, Mater. Sci. Technol., 18 (2002) 1092.
29 Z. H. Zhang, X. F. Bian and Y. Wang, Z. Metallkd., 93 (2002) 585.
30 Z. H. Zhang, X. F. Bian and Y. Wang, J. Cryst. Growth, 243 (2002) 531.
31 Tomiska, Q. Jiang and R. Lück, Z. Metallkd., 84 (1993) 755.